Tensile Cracks in Creeping Solids

February 1979

H. Riedel[1] and J. R. Rice[2]

Abstract. The aim of the paper is to answer the question: which loading parameter determines the stress and strain fields near a crack tip, and thereby the growth of the crack, under creep conditions? As candidates for relevant loading parameters, the stress intensity factor K_I, the path-independent integral C^*, and the net section stress σ_{net} have been proposed in the literature. The answer, which is attempted in this paper, is based on the time-dependent stress analysis of a stationary crack in Mode I tension. The material behavior is modelled as elastic-nonlinear viscous where the nonlinear term describes power law creep. At the time $t=0$ load is applied to the cracked specimen, and in the first instant the stress distribution is elastic. Subsequently, creep deformation relaxes the initial stress concentration at the crack tip, and creep strains develop rapidly near the crack tip. These processes may be analytically described by self-similar solutions for short times t.

An important result of the analysis is that small scale yielding may be defined. In creep problems, this means that elastic strains dominate almost everywhere except in a small 'creep zone' which grows around the crack tip. If crack growth ensues while the creep zone is still small compared with the crack length and the specimen size, the stress intensity factor governs crack growth behavior.

[1]Division of Engineering, Brown University, Providence, R.I. 02912. Permanent affiliation Max-Planck-Institut für Eisenforschung, 4000 Düsseldorf, F.R.G.

[2]Division of Engineering, Brown University, Providence, R.I. 02912.

DISCLAIMER

If, however, the calculated creep zone becomes larger than the specimen size, the stresses become finally time-independent and the elastic strain rates can be neglected. In this limiting case, the stress field is the same as in the fully-plastic limit of power law hardening plasticity which has been treated in the literature. The loading parameter which determines the near tip fields uniquely is then the path-independent integral C^* .

It should be emphasized that K_I and C^* characterize opposite limiting cases. Which case applies in a given situation can be decided by comparing the creep zone size with the specimen size and the crack length. Criteria for small scale yielding are worked out in several alternative forms. Besides several methods of estimating the creep zone size, a convenient expression for a characteristic time is derived also, which characterizes the transition from small scale yielding to extensive creep of the whole specimen.

Key words: fracture mechanics, stress analysis, elevated temperature mechanical properties, creep.

Introduction

Under elevated temperature creep conditions in ductile solids, macroscopic cracks grow by local failure of the highly strained material near the crack tip due to the initiation and joining of microcavities, sometimes aided by local corrosion. These processes are often confined to a small fracture process zone near the crack tip. The aim of the present paper is to analyze the stress and strain fields which encompass the process zone and set boundary conditions on its behavior. In the analysis, the fracture process zone is assumed to be negligibly small. This kind of analysis is necessary to gain insight into the problem of which macroscopic loading parameter governs crack growth under creep conditions. As candidates for relevant loading parameters, the stress intensity factor K_I [1], the net section stress σ_{net} [2], the path independent integral C^* [3,4], and the crack tip opening displacement rate $\dot{\delta}$ [5] have been proposed. For a more comprehensive survey of the recent literature, see references [6-8]. The question of the 'right' loading parameter is far from being academic: if, from laboratory crack growth tests, growth rates in large structures are to be predicted, it may be too conservative to use the stress intensity factor as the correlating parameter. This is clearly demonstrated in the work of Kœrazawa and Mori [9], where the crack growth rate drops by two orders of magnitude if the specimen size is chosen as 20mm instead of 8mm, although the nominal stress intensity factor is kept constant. On the other hand, the use of the net section stress as the correlating parameter between laboratory tests and large structures can lead to dangerous predictions in cases where the stress intensity factor should have been used.

Based on a Dugdale Model, Riedel [8] and Ewing [10] have worked out conditions under which the stress intensity factor is the relevant parameter for creep crack growth. More recently, Riedel [7] has confirmed these results by the analysis of a stationary shear crack (Mode III) in an isotropic material that is capable of elastic and creep deformation everywhere. The key feature of the analysis is that 'small scale yielding' conditions may be defined. In creep problems, small scale yielding means that elastic strains dominate almost everywhere in the specimen except in a small 'creep zone,' which grows around the crack tip. The creep zone boundary has been defined for stationary cracks as the locus where creep strain and elastic strain are equal. If crack growth ensues while the creep zone is still sufficiently small compared with the specimen size, the stress intensity factor governs crack growth.

In the present paper, the stress analysis of a stationary crack under creep conditions is worked out for tensile loading (Mode I). Both small scale yielding as well as the case where the whole specimen creeps extensively ('fully yielded case') are considered. For small scale yielding, the stress intensity factor K_I governs crack growth initiation, whereas the path-independent integral C^* [3,4] is the relevant loading parameter for the case of extensive creep. Finally, it is pointed out that, for growing cracks, K_I and C^* remain the loading parameters, which determine the crack growth rate. But the relation between the crack growth rate and the loading parameter may become complicated, for instance dependent on the previous history of loading and crack growth. The stress analysis of growing cracks will be further discussed in two forthcoming papers [11,12].

Constitutive equations, initial and boundary conditions

We consider the two-dimensional problems of plane stress or plane strain tension, known also as Mode I. A crack is embedded in a material that may be classified as a Maxwell-type elastic-nonlinear-viscous material, where the non-linear behavior represents power law creep. Creep deformation is assumed to be incompressible. The deviatoric strain rate tensor, $\dot{\underline{\varepsilon}}'$ is related to the deviatoric stress and stress rate tensors, $\underline{\sigma}'$ and $\dot{\underline{\sigma}}'$ by: †

$$\dot{\underline{\varepsilon}}' = \frac{1}{2G}\ \dot{\underline{\sigma}}' + \frac{3}{2} B \underline{\sigma}' \sigma_e^{n-1} \quad . \tag{1}$$

Here, G is the elastic shear modulus. The creep exponent n and the temperature-dependent factor B are the parameters of the power law creep relation $\dot{\varepsilon} = B\sigma^n$, measured in uniaxial tension creep tests. The equivalent tensile stress σ_e is given by: †

$$\sigma_e = \left(\frac{3}{2}\ \underline{\sigma}' : \underline{\sigma}'\right)^{1/2} \quad . \tag{2}$$

If elastic compressibility is admitted, the traces of stress and strain tensors are related via the bulk modulus κ :

$$\mathrm{tr}\ \underline{\varepsilon} = \frac{1}{3\kappa}\ \mathrm{tr}\ \underline{\sigma} \ . \tag{3}$$

---

† In the tensor notation used throughout this paper, underlined quantities are tensors. A dot between two tensors indicates summation over one index; a double dot indicates summation over two indices. $\underline{I}$ is the two-dimensional unit tensor; i.e., $\underline{I}:\underline{I} = 2$, $\underline{\nabla}$ is the two-dimensional gradient operator, and ∇^2 is the two-dimensional Laplace-operator. A prime denotes the deviatoric part of a three-dimensional tensor. Traces are the sum of the three diagonal tensor components.

The material law stated in eqs. (1) to (3) is supplemented by the equilibrium condition

$$\underline{\nabla \cdot \sigma} = 0 \tag{4}$$

and by the compatibility relation which, for plane problems, has the form

$$\underline{\nabla} \cdot (\underline{\nabla} \cdot \underline{\varepsilon}') = \frac{2}{3} \nabla^2 (tr\ \underline{\varepsilon}) - \nabla^2 \varepsilon_{33} \quad . \tag{5}$$

In the direction of the crack front (x_3-axis), we have an additional equation, either $\varepsilon_{33} = 0$ (plane strain), or $\sigma_{33} = 0$ (plane stress).

The initial condition is that a load is applied suddenly to the cracked specimen at the time $t=0$. According to the material law stated in eq. (1), the instantaneous response of the material is elastic. Therefore, at time $t=0$, the elastic stress distribution [13] prevails in the cracked body.

Boundary conditions are prescribed on the traction-free crack faces, $\underline{n} \cdot \underline{\sigma} = 0$ ($\underline{n}$ = normal vector on crack face), and at infinity. For small scale yielding (short time response) it suffices to regard the crack as being of semi-infinite extent, with the boundary condition at infinity being the requirement of asymptotic approach to the elastic singular field characterized by the stress intensity factor [13].

The problem stated in the preceding eqs. (1-5) will now alternately be formulated in terms of the Airy stress function, ϕ. It is related to the stress tensor by

$$\underline{\sigma} = -\underline{\nabla\nabla}\phi + \underline{I}\nabla^2\phi \tag{6}$$

thus automatically fulfilling the equilibrium condition (4). Inserting the stress tensor according to eq. (6) into the material law (eqs. 1-3) and inserting the resulting strain rate tensor into the compatibility condition (eq. 5), one arrives at an equation for the Airy stress function ϕ .

For plane strain, the deviatoric stress component σ'_{33} cannot be expressed in terms of ϕ ; the plane strain condition $\epsilon_{33} = 0$ forms an additional equation. Thus, for plane strain we have two coupled equations for ϕ and σ'_{33} :

$$2\,\frac{1-\nu}{E}\,\nabla^2\left(\nabla^2\dot{\phi}+\dot{\sigma}'_{33}\right) - B\underline{\nabla}\cdot\{\underline{\nabla}\cdot[(\underline{I}(\nabla^2\phi-\sigma'_{33}) - 2\underline{\nabla}\underline{\nabla}\phi)\sigma_e^{\,n-1}]\} = 0 \qquad (7a)$$

$$\left(\frac{1-2\nu}{3E}\,\nabla^2\dot{\phi} + \frac{1}{E}\,\dot{\sigma}'_{33}\right) + B\sigma'_{33}\sigma_e^{\,n-1} = 0\ . \qquad (7b)$$

Here, E is Young's modulus, ν is Poisson's ratio, and a dot means time derivative. The equivalent stress σ_e is given in terms of ϕ and σ'_{33} as

$$\sigma_e = \frac{\sqrt{3}}{2}\,\{2(\underline{\nabla}\underline{\nabla}\phi:\underline{\nabla}\underline{\nabla}\phi) - (\nabla^2\phi)^2 + 3\sigma'^{\,2}_{33}\}^{1/2}\ . \qquad (8)$$

For incompressible material $(\nu\to 1/2)$, eq. (7) is simplified since $\sigma'_{33} = 0$.

For plane stress the governing equation for the Airy stress function has the form

$$\frac{2}{E}\,\nabla^4\dot{\phi} - B\underline{\nabla}\cdot\{\underline{\nabla}\cdot[(\underline{I}\nabla^2\phi - 3\underline{\nabla}\underline{\nabla}\phi)\sigma_e^{\,n-1}]\} = 0 \qquad (9)$$

and the equivalent stress is

$$\sigma_e = \frac{1}{\sqrt{2}} \left[3(\underline{\nabla\nabla}\phi : \underline{\nabla\nabla}\phi) - (\nabla^2\phi)^2\right]^{1/2} \quad . \tag{10}$$

We use either a polar coordinate system (r,θ) with $\theta=0$ directly ahead of the crack and the origin at the crack tip, or cartesian coordinates (x,y) with the x-direction parallel to $\theta=0$.

The equations for ϕ , (eqs. 7 and 9), together with the expressions for σ_e are non-linear partial differential equations of fifth order with three independent variables: r , θ , t . Because of the complexity of the equations, no closed-form solutions can be expected, in general. On the other hand, numerical methods have particular stability problems with the rapid stress redistribution near crack tips in strongly non-linear elasto-viscous materials. We show here however, that an approximate, but rather complete, picture of the stress and strain fields can be achieved by analytical methods. In the following sections, first the asymptotic behavior near the crack tip is studied, which is common to the small scale yielding and the fully yielded case, and to intermediate cases. Then the fully yielded case follows which is relatively simple, and finally the small scale yielding case, which is more complicated, is treated by means of self-similar solutions.

The asymptotic field near the crack tip

Near the crack tip $(r\to 0)$, the elastic strain rates can be neglected in the material law, eq. (1), compared with the creep rates. The reason is that the creep exponent usually is greater than 1 (n = 4 to 6 is typical), which makes the creep rates $(\propto\sigma^n)$ much larger than the elastic strain rates $(\propto\dot{\sigma})$, if the stress near the crack tip is unbounded.

As a consequence, the linear terms in the partial differential equations (7 and 9) can be neglected for $r \to 0$. This leads to exactly the same asymptotic problem which is known from the analysis of rate-insensitive "power law" strain-hardening materials. Hutchinson [14] and Rice and Rosengren [15] (referred to as HRR hereafter) have given the form of the stress and strain singularities:

$$\underline{\sigma}(r,\theta,t) = A(t)\tilde{\underline{\sigma}}(\theta)r^{-1/(n+1)} \quad . \tag{11}$$

The creep strain and strain rate has an $r^{-n/(n+1)}$ singularity. The angular functions $\tilde{\underline{\sigma}}(\theta)$ are given graphically in refs. [14-17]. Here, we understand $\tilde{\underline{\sigma}}(\theta)$ normalized as in [17], such that the function, $\tilde{\sigma}_e(\theta)$, which belongs to the equivalent stress, is normalized to unity at its maximum value. The amplitude, A , of the HRR-stress field is a function of the time and of the applied load. It cannot be specified by analyzing the asymptotic problem alone. In the deformation theory of power-law hardening plasticity, the amplitude of the HRR-field could be specified by means of the J-integral [14,15]. Analogously, the amplitude of the HRR-field will be specified in terms of the C^*-integral for the limiting case of extensive creep of the whole specimen (see next section). This case corresponds to steady-state creep, thus elastic strain rates vanish and the material responds as if it were purely viscous. For small scale yielding, however, the elastic as well as the creep strain rates are important. Neither J nor C^* are then path-independent, and approximate methods must be applied to determine the amplitude $A(t)$.

Extensive creep of the whole specimen

The material law stated in eq. (1) has the property that the stresses become time-independent ($\dot{\underline{\sigma}} \to 0$) after long times ($t \to \infty$) if the load is kept constant and geometry changes can be neglected. This latter condition, in particular, implies that the crack must be effectively stationary. So, for $\dot{\underline{\sigma}} = 0$, the constitutive equations (1)-(5) take the form of non-linear elastic materials, if the strain rate is replaced by strain. The same non-linear elastic material law also describes the fully plastic limit for power law hardening materials. This case has been studied extensively in the literature [18-22] and the results can immediately be used here by writing strain rate instead of strain, and the path-independent integral C^* [3,4] instead of the J-integral [13]. The C^*-integral can be measured at the loading pins of cracked specimens [3]. Its relation to the applied load has also been calculated numerically, reading C^* instead of J in refs. [18-22]. On the other hand, C^* is related to the amplitude of the near tip singular field [14,15] by

$$A(t \to \infty) = \left[\frac{C^*}{BI_n}\right]^{1/(n+1)} \tag{12}$$

In plane strain, numerical values of the factor I_n range from 3.8 (for $n=\infty$) to 6.3 (for $n=1$)[17]. Plane stress values of I_n are 2.87 (for $n=13$) and 3.86 (for $n=3$)[16].

According to eq. (12), C^* is the loading parameter which determines the near-tip singular field, and thereby the initiation of crack growth, if the whole specimen creeps extensively.

Small scale yielding

In a previous paper [7] it has been shown that small scale yielding can be defined under creep conditions. The small scale yielding solution is valid as long as the creep zone is sufficiently small compared with the dimensions of the specimen. It may also be called a short-time solution, since it describes the development of stresses and strains shortly after the load is applied at $t=0$.

The solution of the small scale yielding problem is now shown to be possible in terms of self-similar functions. It follows the same lines as in the Mode III case [7], and also the nature of the time-dependence of stresses and strains is the same.

Observe that the stress field $\underline{\sigma}$ at any point r,θ at (short) time t after load application is a function of the following set of variables and material parameters:

$$r,\theta,t\ ,\ K_I\ ,\ E\ ,\ B\ ,\ \nu\ ,\ n\ .$$

Further, from the form of the differential equations (7,9) for ϕ , and hence for the stress field, it is clear that E , B , and t can enter only as the product EBt , and we note that $(EBt)^{-1/(n-1)}$ has the same physical dimensions as does stress. Accordingly, from standard considerations of dimensional consistency, the stress field $\underline{\sigma}$ for small scale yielding, or short times, has the form

$$\underline{\sigma} = (EBt)^{-1/(n-1)}\underline{F}[(EBt)^{-2/(n-1)}r/K_I^2\ ,\ \theta\ ,\ n\ ,\ \nu]$$

where $\underline{F}$ is a dimensionless function of its (dimensionless) arguments.

In fact, for plane stress the function $\underline{F}$ is independent of ν, since ν appears in neither the differential equation (9) nor the boundary conditions. The detailed formulation of a solution in the above "self-similar" form is discussed next, introducing notations paralleling those of [7].

Self-similar solutions. For plane strain, the self-similar stress function and stress component σ'_{33} that satisfy eq. (7) as well as the initial and boundary conditions have the form

$$\phi(r,\theta,t) = \frac{E}{1-\nu}\frac{1}{(2\pi)^2}\left[\frac{(1-\nu)K_I}{E}\right]^4 \phi(R,\theta)T^{3/(n-1)} \tag{13a}$$

$$\sigma'_{33}(r,\theta,t) = \frac{E}{1-\nu}\Sigma'_{33}(R,\theta)T^{-1/(n-1)} \quad . \tag{13b}$$

The dimensionless time T and radial coordinate R are given by

$$T = \frac{n-1}{2}\left(\frac{E}{1-\nu}\right)^n Bt \tag{14}$$

$$R = \frac{r}{\frac{1}{2\pi}\left[\frac{(1-\nu)K_I}{E}\right]^2 T^{2/(n-1)}} \quad . \tag{15}$$

The dimensionless shape functions ϕ and Σ'_{33} obey the following differential equations (where the operator $\underline{\nabla}$ is now understood to act in the dimensionless (R,θ) coordinate system):

$$-2\nabla^2\left(\frac{1}{2} + R\frac{\partial}{\partial R}\right)\left(\nabla^2\phi+\Sigma'_{33}\right) + \underline{\nabla}\cdot\{\underline{\nabla}\cdot[\left(2\underline{\nabla}\underline{\nabla}\phi - \underline{I}(\nabla^2\phi-\Sigma'_{33})\right)$$

$$\left(\frac{3}{2}(\underline{\nabla}\underline{\nabla}\phi:\underline{\nabla}\underline{\nabla}\phi) - \frac{3}{4}(\nabla^2\phi)^2 + \frac{9}{4}\Sigma'^2_{33}\right)^{(n-1)/2}]\} = 0 \ , \tag{16a}$$

$$-\left(\frac{1}{2} + R\frac{\partial}{\partial R}\right)\frac{(1-2\nu)\nabla^2\phi + 3\Sigma'_{33}}{3(1-\nu)}$$

$$+ \Sigma'_{33}\left[\frac{3}{2}(\nabla\nabla\phi:\nabla\nabla\phi) - \frac{3}{4}(\nabla^2\phi)^2 + \frac{9}{4}\Sigma'^2_{33}\right]^{(n-1)/2} = 0 \ . \qquad (16b)$$

For plane stress the same form for ϕ as defined by eqs. (13a, 14 and 15) may be assumed, but with $1-\nu$ replaced everywhere by 1 . In this case, eq. (9) reduces to

$$-2\nabla^2\left(\frac{1}{2} + R\frac{\partial}{\partial R}\right)\nabla^2\phi + \nabla\cdot\left\{\nabla\left[(3\nabla\nabla\phi - \underline{1}\nabla^2\phi)\right.\right.$$

$$\left.\left.\left(\frac{3}{2}(\nabla\nabla\phi:\nabla\nabla\phi) - \frac{1}{2}(\nabla^2\phi)^2\right)^{(n-1)/2}\right]\right\} = 0 \ . \qquad (17)$$

The boundary condition at infinity is the elastic field. In dimensionless form:

$$\phi(R\to\infty) = \frac{4}{3}R^{3/2}\cos^3\frac{\theta}{2} \ . \qquad (18a)$$

For plane strain, we also have the boundary condition

$$\Sigma'_{33}(R\to\infty) = -\frac{2}{3}(1-2\nu)R^{-1/2}\cos\frac{\theta}{2} \ . \qquad (18b)$$

Once the shape functions ϕ and Σ'_{33} are known by solving the differential equations (16) and (17), subject to traction-free crack surface boundary conditions, stresses and strains can be calculated. The stress tensor has the form

$$\underline{\sigma} = \frac{E}{1-\nu}T^{-1/(n-1)}\underline{\Sigma}(R,\theta) \ , \qquad (19)$$

where the in-plane components of the dimensionless shape function follow from ϕ :

$$\underline{\Sigma} = -\nabla\nabla\phi + \underline{I}\,\nabla^2\phi \quad . \tag{20}$$

The factor $1-\nu$ must be replaced by unity for plane stress. Further, from eq. (11) it is known that $\underline{\Sigma}$ must become infinite in the form $R^{-1/(1+n)}$ as $R \to 0$. The elastic strain, $\underline{\varepsilon}^{el}$, follows from eq. (19) by Hooke's law. The creep strain, $\underline{\varepsilon}^{cr}$, can also be expressed in terms of $\underline{\Sigma}$, using eq. (1):

$$\underline{\varepsilon}^{cr} = T^{-1/(n-1)}\underline{E}^{cr}(R,\theta) \tag{21}$$

with

$$\underline{E}^{cr}(R,\theta) = \frac{3}{2\sqrt{R}}\int_R^\infty \underline{\Sigma}'\left(\frac{3}{2}\,\underline{\Sigma}':\underline{\Sigma}'\right)^{(n-1)/2}\frac{d\rho}{\sqrt{\rho}} \quad . \tag{22}$$

Here, $\underline{\Sigma}' = \underline{\Sigma}'(\rho,\theta)$ is the deviatoric part of $\underline{\Sigma}$ and the integral on ρ is done with θ fixed. The total strain, $\underline{\varepsilon}$, is given by the sum $\underline{\varepsilon} = \underline{\varepsilon}^{el} + \underline{\varepsilon}^{cr}$.

A precise graphical presentation of the stress and strain fields would require the numerical solution of the non-linear partial differential equations (16) and (17), which will be attempted in future work, in analogy to the solutions obtained in Mode III [7].

Approximate description of the small scale yielding stress and strain fields. Presently, no numerical solutions of equations (16) and (17) are available, but a qualitative description of the stress and strain fields is possible. First we note that the time dependence of the stresses and strains (eqs. 19-22) is the same as in Mode III [7]: the initial elastic stress concentration at the crack tip is relaxed by creep deformation and the stresses are distributed more homogeneously across the specimen, while creep strains develop prefereably in a creep zone which grows around the crack tip.

Using eqs. (11) and (19), we know the r and t dependence of the near-tip HRR-field, which can now be specified except for a numerical amplitude factor α_n. (This factor will be calculated approximately in the next sub-section, where we show $\alpha_n \approx 1$). Thus the near tip stress and strain fields, for small scale yielding, are

$$\underline{\sigma} = \alpha_n \left[\frac{nK_I^2}{\pi(n+1)^2 EB}\right]^{1/(n+1)} \tilde{\underline{\sigma}}(\theta)(rt)^{-1/(n+1)} \tag{23}$$

$$\underline{\varepsilon} = \frac{3}{2} B(n+1)\alpha_n^n \left[\frac{nK_I^2}{\pi(n+1)^2 EB}\right]^{n/(n+1)} \tilde{\underline{\sigma}}'(\theta)[\tilde{\sigma}_e(\theta)]^{n-1} \frac{t^{1/(n+1)}}{r^{n/(n+1)}} \quad . \tag{24}$$

So we know the asymptotic fields at infinity (linear elastic field) and near the crack tip (HRR-field, eqs. (23) and (24)). One can now assemble approximate solutions by simply extrapolating the asymptotic fields to the locus $r_1(\theta,t)$ which is defined by the equality of the equivalent stresses of the remote elastic and the near tip HRR-field. This definition leads

to

$$r_1(\theta,t) = \frac{1}{2\pi}\left(\frac{K_I}{E}\right)^2\left[\frac{(n+1)^2 E^n B t}{2n\alpha_n^{n+1}}\right]^{2/(n-1)} F_1(\theta) \qquad (25)$$

with the angular function

$$F_1(\theta) = \left\{\frac{\cos^2\frac{\theta}{2}\left[(1-2\nu)^2 + 3\sin^2\frac{\theta}{2}\right]}{\left[\tilde{\sigma}_e(\theta)\right]^2}\right\}^{(n+1)/(n-1)} . \qquad (26)$$

This form applies for plane strain; for plane stress, the expression $1-2\nu$ must be replaced by unity, and $\tilde{\sigma}_e(\theta)$ and α_n have their plane stress values.

The creep zone boundary has been defined by equating the equivalent creep strain ε_e^{cr} to the equivalent elastic strain ε_e^{el} [7] . If we use this definition and calculate the strains from the assembled stress field described above, the result for the creep zone boundary $r_{cr}(\theta,t)$ has the same functional form as r_1 except for the angular function $F_{cr}(\theta)$:

$$r_{cr}(\theta,t) = \frac{1}{2\pi}\left(\frac{K_I}{E}\right)^2\left[\frac{(n+1)^2 E^n B t}{2n\alpha_n^{n+1}}\right]^{2/(n-1)} F_{cr}(\theta) . \qquad (27)$$

According to eq. (27) the creep zone expands in proportion to $t^{2/(n-1)}$. The angular functions $F_1(\theta)$ and $F_{cr}(\theta)$ are shown in Fig. 1. Within the accuracy of the present method, the creep zone boundary runs into the crack tip. More accurate methods, however, might lead to a creep zone boundary which hits the crack faces behind the crack tip.

Approximate calculation of the factor α_n . The proper way to calculate the dimensionless factor α_n , which appears in the results of

the preceding subsection, would be to solve the partial differential equations (16) and (17) numerically; the amplitude of the near tip singular field is then part of the result. In the present paper, however, we estimate the value of α_n by means of the path-integral J [13]. The quantity $W = \int \underline{\sigma} : d\underline{\varepsilon}$, which appears in the J-integral, is understood as an integral over the deformation history at each material point. With this definition of W , the J-integral is, in general, path-dependent for creep problems. We assume, however, that J is approximately path-independent. The reason why we regard this as a reasonable approximation is the following: creep straining takes place mainly in the creep zone. In this region, the HRR-field is a good approximation which becomes asymptotically exact as $r \to 0$. Further, we find that it is possible to eliminate both coordinates (r,θ) from eqs. (23) and (24), thus showing that stresses and strains in the HRR-region behave as if there were a unique relationship $\varepsilon(\sigma)$, independent of (r,θ) at any instant of time:

$$\underline{\varepsilon} = \frac{3}{2} B(n+1) t \underline{\sigma}' \sigma_e^{n-1} \quad . \tag{28}$$

The existence of a unique stress-strain relation, however, implies path-independence of J .

For the HRR-field, the value of the J-integral has been calculated [17,18] as

$$J_o = (n+1) B t I_n [A(t)]^{n+1} \quad . \tag{29}$$

In the elastic field, J has the well known value [13]:

$$J_\infty = \begin{cases} K^2(1-\nu^2)/E & \text{for plane strain} \\ K^2/E & \text{for plain stress} \end{cases} . \qquad (30)$$

Assuming approximate path-independence of J (i.e. $J_o \approx J_\infty$) we obtain the amplitude of the singularity

$$A(t) \approx \left[\frac{K_I^2(1-\nu^2)/E}{(n+1)BI_n t}\right]^{1/(n+1)} \qquad (31)$$

and, with the definition of α_n according to eqs. (11) and (23),

$$\alpha_n \approx \left[\frac{n+1}{n}\ \frac{\pi(1-\nu^2)}{I_n}\right]^{1/(n+1)} . \qquad (32)$$

This form is for <u>plane strain</u>. Numerical values are $\alpha_3 = .912$ and $\alpha_{13} = .975$ for $\nu = 0.3$. For <u>plane stress</u> the factor $(1-\nu^2)$ must be deleted, and the plane stress value for the integral I_n [16] must be inserted. Numerical values are $\alpha_n = 1.015$ independent of n , within 1/2 percent accuracy.

It is interesting to note that with this approximate value of α_n , eq. (32), the near tip fields of $\underline{\sigma}$ and $\underline{\dot{\varepsilon}}$ for small scale yielding have the same form as for the extensive yielding case (eqs. (11) and (12)), provided that C^* , which governs the amplitude of the latter case, is replaced in all formulae by $G/(1+n)t$. Here $G = (1-\nu^2)\ K_I^2/E$ for plane strain and K_I^2/E for plane stress.

<u>Assessment of the accuracy</u>. Unfortunately, the error of the approximations in the previous two sub-sextions can hardly be estimated

analytically. Therefore, we apply the approximate method to Mode III and compare the results with the numerical results which are there available [7]. It turns out that the approximate method under-estimates the amplitude of the HRR-field for $n \leq 5$ by 5, 15, 30 percent for $n = 4,3,2$, respectively. For $n \geq 5$, the approximate method over-estimates the result by a maximum of 10% (for $n=\infty$). The practical range of creep exponents is $n = 4$ to 6 and sometimes higher; in this range the approximation is very close to the exact Mode III result. On the other hand, as $n \to 1$ the concept of a growing creep zone becomes ill-defined and this may result in the inaccuracy of the approximation at low n. Figure 2 shows a comparison between the numerically calculated stress and the approximately calcuated stress which is composed of the HRR-field near the crack tip and the elastic field far from the crack tip. With the strains calculated from this stress field, one obtains a creep zone size which coincides within 20 percent accuracy with the value calculated numerically [7].

In conclusion, the approximate methods work well for Mode III, and we proceed assuming their approximate validity for Mode I, too.

Criteria for small scale yielding vs. extensive creep of whole specimen

From the preceding analysis it is clear that the stress intensity factor K_I and the integral C^* characterize the near tip field--and thereby crack growth behavior--in opposite limiting cases: a description by K_I applies if the crack grows while the specimen behaves predominantly elastic except in a creep zone which is small compared with the specimen size (brittle failure); the C^*-integral applies if crack growth is accompanied by extensive creep of the whole specimen (ductile behavior).

As an example, we calculate the crack growth initiation time as a function of the loading parameter. We assume that the crack starts to

grow once a critical equivalent strain, ε_c, is attained at a small structural distance, r_c, from the crack tip. For plane stress r_c is defined directly ahead of the crack $(\theta=0)$, and for plane strain it is measured in the direction where $\tilde{\sigma}_e(\theta)$ is a maximum. The near tip strains are given by eq. (24) for small scale yielding. Inverting eq. (24) one obtains the crack growth initiation time, t_i, as a function of the stress intensity factor:

$$t_i = \varepsilon_c^{n+1} \frac{1}{E^n B(n+1)} \left[\frac{n+1}{2n\alpha_n^{n+1}} \frac{2\pi E^2 r_c}{K_I^2} \right]^n . \tag{33}$$

If extensive creep of the whole specimen precedes crack growth initiation, the strains are given by inserting eqs. (11) and (12) into eq. (1). Then the initiation time depends on C^*

$$t_i = \varepsilon_c^{-1/(n+1)} B^{-1/(n+1)} \left[\frac{I_n r_c}{C^*} \right]^{n/(n+1)} . \tag{34}$$

Now some practical guidelines will be discussed as to how one can decide whether or not small scale yielding conditions prevail in a given test situation:

(1) A direct approach would be to estimate the creep zone size experimentally, e.g., by observation of a polished specimen surface near the crack tip.

(2) The second possibility would be to calculate the creep zone size from eq. (27) and compare it with the specimen size. Since the material parameters B and n play an important role in eq. (27), this formula is strictly limited to power law creep.

(3) A formula for the creep zone size, which will be approximately valid for more general creep laws than pure power-law creep, is obtained if the time in eq. (27) is replaced by any one of the strain components, ε_{ij} . Using eq. (24) with eq. (27) leads to

$$r_{cr}(\theta,t) = \beta_n(\theta_o) \left[\frac{\sqrt{6\pi}\ \varepsilon_{ij}(r,\theta_o,t) r^{n/(n+1)}}{(K_I/E)}\right]^{2(n+1)/(n-1)} F_{cr}(\theta) \qquad (35a)$$

with the numerical factor β_n

$$\beta_n = \left[\frac{n+1}{3^{3/2} n\, \alpha_n^{n+1}\, \tilde{\sigma}_{ij}(\theta_o)\sigma_e^{n-1}(\theta_o)}\right]^{2(n+1)/(n-1)} . \qquad (35b)$$

In eqs. (35), the strain component ε_{ij} is supposed to be measured at a position (r,θ_o) by means of a high temperature strain gauge. The position (r,θ_o) must be within the creep zone; θ_o is an arbitrary angle and the result of eq. (35a) is independent of θ_o . For plane stress, it will be convenient to measure $\varepsilon_{\theta\theta}$ directly ahead of the crack tip $(\theta_o=0)$. For plane strain, larger tensile strains can be measured above the crack tip $(\theta_o=\pi/2)$ with the axis of the strain gauge oriented at an angle $\theta=3\pi/4$. Then numerical values for β_n are $\beta_3 = 0.212$ and $\beta_{13} = 0.238$ for plane strain, and $\beta_3 = .074$ and $\beta_{13} = .067$ for plane stress. Thus, eqs. (35) provide a rough estimate for the creep zone size even if the creep exponent n is uncertain, since the result in this form is not strongly dependent of n , if n is large.

(4) The creep zone size can also be expressed in terms of crack opening displacement (COD) , δ , which is sometimes convenient to

measure. The resulting relation depends on the definition of COD: one definition of COD is to measure the distance between the two crack faces at the point where the creep zone boundary hits the crack faces behind the crack tip. With the approximations of the present theory, this point cannot be determined (see Fig. 1), but the relation between r_{cr} and δ_{czb} (= COD at the creep zone boundary) must have the form

$$r_{cr} = \beta_n' \left[\frac{E\delta_{czb}}{K_I}\right]^2 F_{cr}(\theta) \quad . \tag{36}$$

The factor β_n' can only be estimated by analogy with the Mode III case [7]. The result is $\beta_n' F_{cr}(\frac{\pi}{2}) \approx 0.3$. The advantage of eq. (36) is that it allows an estimate of the creep zone size independently of the creep parameters B and n . So it may be suspected that eq. (36) is approximately valid for more general creep laws than pure power-law creep. A practical drawback of eq. (36) is that COD at the creep zone boundary will be hard to measure precisely.

COD can also be defined at the point where the line $\theta = 135°$ originating from the apex of the crack profile, intersects the crack profile [23]. This COD value will be denoted by δ_t . With this definition of COD, we obtain

$$r_{cr} = \beta_n'' \left[\frac{\delta_t}{8}\left(\frac{E}{K_I}\right)^2\right]^{2/(n-1)} \left[\frac{E\delta_t}{K_I}\right]^2 F_{cr}(\theta) \tag{37a}$$

with

$$\beta_n'' = \frac{1}{16}\left[\frac{n+1}{n} \cdot \frac{(2\pi)^{1/2}}{|\tilde{u}_\theta(\pi)|\alpha_n^{n+1}}\right]^{2(n+1)/(n-1)} \quad . \tag{37b}$$

The angular part, $\tilde{u}_\theta(\theta)$, of the displacement function is

$$\tilde{u}_\theta(\theta) = \frac{3}{2}\frac{n+1}{n}\left\{\frac{1}{2}(n+1)\frac{\partial}{\partial\theta}\left[\left(\tilde{\sigma}_{rr} - \tilde{\sigma}_{\theta\theta}\right)\tilde{\sigma}_e^{n-1}\right] - 2\tilde{\sigma}_{r\theta}\tilde{\sigma}_e^{n-1}\right\}. \tag{37c}$$

Typical numerical values are for plane strain: $\beta_3'' = 0.63$, $\beta_5'' = 0.40$, $\beta_{13}'' = 0.32$, and for plane stress: $\beta_3'' = 0.127$, $\beta_5'' = 0.116$, $\beta_{13}'' = 0.108$.

(5) Finally, the characteristic time for the transition from small scale yielding to extensive creep of the whole specimen can be estimated analytically. Figure 3 shows the time-dependence of the amplitude $A(t)$, of the near tip singular stress field. The short-time limit is given by the small scale yielding result (eq. (31)) and the long-time is given by eq. (12). The characteristic time, t_1 , for the transition defined in Fig. 3, is

$$t_1 = \frac{K_I^2(1-\nu^2)/E}{(n+1)\ C^*} \tag{38}$$

for plane strain; for plane stress, replace $1-\nu^2$ by 1 . Small scale yielding prevails if the time is sufficiently small compared with the characteristic time t_1 . In eq. (38), C^* is considered as a quantity which is known from a numerical analysis of a non-linear viscous (or, by analogy, small strain non-linear elastic) problem [18-22]. For a center-cracked strip, for instance, Goldman and Hutchinson [18] give

$$C^* = a\sigma_\infty\dot{\varepsilon}_\infty^{cr}\left(\frac{2}{\sqrt{3}}\right)^{n+1}\hat{J}\left(\frac{a}{b}, n\right) . \tag{39}$$

The crack length is $2a$, the strip width is $2b$; $\hat{J}$ is given graphically in ref. [18] as a function of a/b and of the creep exponent n; σ_∞ and $\dot{\varepsilon}_\infty^{cr}$ are the remotely applied stress and creep strain rate. The material parameter B does not appear in eqs. (38) and (39), but the creep exponent n has a significant influence both on $\hat{J}$ [18] and on eq. (38). With eq. (39) the transition time is given by

$$t_1 = \frac{\sigma_\infty}{E\dot{\varepsilon}_\infty^{cr}} \frac{(\sqrt{3}/2)^{n-1}}{1+n} \frac{\hat{J}(a/b,1)}{\hat{J}(a/b,n)} \quad . \tag{40}$$

According to eq. (27), the creep zone size at the time t_1 is approximately 1/10 of the half crack length, a.

Discussion

Apart from the approximations which are involved in the analysis of the small scale yielding case, further limitations of the present theory must be kept in mind.

Firstly, the theory has been worked out for a material law which, besides elastic deformation, allows for pure power-law creep only. However, the general conclusion, that a creep zone near the crack tip can be defined, will not be altered if more general creep laws are valid, as long as the creep rate increases stronger than linearly as a function of the stress. From the form of the equations (35)-(38), it is expected that the size of the creep zone can be estimated even if the creep law is different from a pure power-law relation. In this connection, we remark in passing that the solution which we have presented for small scale yielding is also valid for creep laws which include, approximately, transient effects through a time-hardening expression of the form

$\dot{\epsilon} = \dot{\sigma}/E + B(t)\sigma^n$, provided that the product Bt in our solution is everywhere replaced by $\int_0^t B(\tau)d\tau$.

Secondly, the theory is based on the assumption that the fracture process zone is always negligibly small compared with the creep zone and the specimen dimensions. In very ductile materials and small specimens, however, the fracture process zone may spread over the whole cross section of the cracked specimen. This situation can no longer reasonably be described by power law creep. The stress and strain distribution in the net section is likely to be more homogeneous in such a situation than predicted by the present theory. Under these conditions, the net section stress could be the loading parameter to determine the life-time of cracked as well as uncracked specimens.

Thirdly, the theory does not cover the range between small scale yielding and extensive creep of the whole specimen. One might expect that an interpolation between the two limiting cases is particularly doubtful for a large plate with a small center-crack under tension. In this case, the creep zone size at the transition time t_1 is about 1/10 of the half crack length. This first appears to be far away from extensive creep of the whole plate. However, if one estimates the strain rates at the transition time by simply adding the remotely applied creep rate $\dot{\epsilon}_\infty^{cr} = B\sigma_\infty^n$, to the creep rate obtained for small scale yielding, it turns out that the elastic strain rates are considerably smaller than the creep rates everywhere except near the creep zone boundary where they are of equal order of magnitude. The condition for the extensive creep limit to be valid is that the creep rates are much larger than the elastic rates everywhere. This starts being fulfilled at the transition time. Hence, there is no big gap between the validity of the small scale yielding and

the extensive creep case. Of course, if a higher degree of accuracy is required, the limiting cases are separated by a period of time where neither of them is accurate enough.

Finally, the analysis has been confined to stationary cracks. For growing cracks, the conclusions concerning the applicability of K_I and C^* are not fundamentally altered, but the situation becomes more complicated. The singular field immediately at the tip of a growing crack can no longer be the HRR-field when elastic effects are present [11]. As a consequence, the influence of the loading parameters on the near tip strains becomes more complicated than for instance the one given in eq. (24). In addition, the stress and strain fields become dependent on the prior history of the loading parameter and of the crack growth. This will be discussed in greater detail in a forthcoming paper [12].

Conclusions

An important result of the stress analysis is that a creep zone near the crack tip can reasonably be defined and calculated. The size in relation to specimen size and crack length determines which loading parameter governs crack growth initiation and growth rates. In large cracked specimens or structures (crack length and specimen size are large compared with the creep zone), the stress intensity factor is the loading parameter which correlates crack growth rates between specimens of different shape. In specimens that are small compared with the creep zone, but large compared with the fracture process zone, the path-independent integral C^* is the relevant loading parameter. If the ligament width of the specimen becomes comparable with the size of the fracture process zone--which has been neglected in the present analysis--the net section stress possibly determines the life-time of a specimen. Excessive crack

tip blunting will have a similar effect.

Criteria for small scale yielding have been developed. They are either based on the comparison of specimen size and creep zone size or on the comparison of the test duration with a characteristic time which can be calculated analytically.

Acknowledgement

H. Riedel was supported in this work by the Max-Planck-Gesellschaft, Munich, and by a visiting appointment in the NSF Materials Research Laboratory at Brown University; J. R. Rice was supported by DOE Contract EY-76-S-02-3084 with Brown University. Helpful discussions with Mr. W. Drugan of Brown University are gratefully acknowledged. We would also like to thank Dr. C. F. Shih of General Electric Research Laboratory and Mr. C. Y. Hui of Harvard University who provided numerical tables of the functions $\tilde{\underline{\sigma}}(\theta)$.

References

[1] Robson, K., "Crack Growth in Two Carbon Steels at 450°C," International Conference on Creep Resistance in Steel, Verein Deutscher Eisenhuttenleute, Dusseldorf, 1972.

[2] Harrison, C.B. and Sandor, G.N., Engineering Fracture Mechanics, Vol. 3, 1971, pp. 403-420.

[3] Landes, J.D. and Begley, J.A., "A Fracture Mechanics Approach to Creep Crack Growth," Mechanics of Crack Growth, ASTM STP 590, American Society for Testing and Materials, 1976, pp. 128-148.

[4] Nikbin, K.M., Webster, G.A., and Turner, C.E., "Relevance of Nonlinear Fracture Mechanics for Creep Cracking," Cracks and Fracture, ASTM STP 601, American Society for Testing and Materials, 1976, pp. 47-62.

[5] Haigh, J.R., Materials Science and Engineering, Vol. 20, 1975, pp. 213-224.

[6] Sadananda, K. and Shahinian, P., Fracture Mechanics; Editors: N. Perrone, H. Liebowitz, D. Mulville, and W. Pilkey, University Press of Virginia, Charlottesville, 1978, pp. 685-703.

[7] Riedel, H., Zeitschrift fur Metallkunde, Vol. 69, No. 12, 1978, pp. 755-760.

[8] Riedel, H., Materials Science and Engineering, Vol. 30, 1977, pp. 187-196.

[9] Koterazawa, R. and Mori, T., Trans. ASME, Journal for Engineering Materials and Technology, Oct. 1977, p. 298.

[10] Ewing, D.J.F., International Journal of Fracture, Vol. 14, 1978, p. 101.

[11] Riedel, H. and Hui, C. Y., to be published.

[12] Riedel, H., research in progress.

[13] Rice, J.R., "Mathematical Analysis in the Mechanics of Fracture," in Fracture: An Advanced Treatise, H. Liebowitz, Ed., Vol. 2, Academic Press, New York, 1968.

[14] Hutchinson, J.W., Journal of Mechanics and Physics of Solids, Vol. 16, 1968, No. 1, pp. 13-31.

[15] Rice, J.R., and Rosengren, G.F., Journal of Mechanics and Physics of Solids, Vol. 16, 1968, No. 1, pp. 1-12.

[16] Hutchinson, J.W., Journal of Mechanics and Physics of Solids, Vol. 16, 1968, No. 5, pp. 337-347.

[17] Shih, C.F., "Small-Scale Yielding Analysis of Mixed Mode Plane-Strain Crack Problems," Fracture Analysis, ASTM STP 560, American Society for Testing and Materials, 1974, pp. 187-210.

[18] Goldman, N.L. and Hutchinson, J. W., International Journal of Solids and Structures, Vol. 11, 1975, pp. 575-591.

[19] Parks, D. M., "Virtual Crack Extension: A General Finite Element Technique for J-Integral Evaluation," Numerical Methods in Fracture Mechanics, A. R. Luxmoore and D. R. J. Owen, Eds., Department of Civil Engineering, University College of Swansea, Jan. 1978.

[20] Ranaweera, M. P. and Leckie, F. A., "Solution of Nonlinear Elastic Fracture Problems by Direct Optimization," Numerical Methods in Fracture Mechanics, A. R. Luxmoore and D. R. J. Owen, Eds., Department of Civil Engineering, University College of Swansea, Jan. 1978, pp. 450-463.

[21] Hutchinson, J. W., Needleman, A., and Shih, C. F., "Fully Plastic Crack Problems in Bending and Torsion," Fracture Mechanics, N. Perrone, H. Liebowitz, D. Mulville and W. Pilkey, Eds., University Press of Virginia, Charlottesville, 1978, pp. 515-528.

[22] A Plastic Fracture Handbook, C.F. Shih et al., Eds., General Electric Research Laboratory, in preparation.

[23] Tracey, D. M., Trans. ASME Journal of Engineering Materials and Technology, Vol. 98, April 1976, pp. 146-151.

sm

Figure Captions

Figure 1. Polar diagrams of the angular functions $F_I(\theta)$ (dashed lines) and $F_{cr}(\theta)$ (solid lines), for plane strain (upper half) and plane stress (lower half). Creep exponent $n=3,4,13$. Poisson's ratio $\nu = 0.3$.

Figure 2. Stress component $\Sigma_{\theta 3}$ vs. distance from crack tip, R, for Mode III, normalized as in eqs. (13)-(15) but with 2G instead of $E/(1-\nu)$. Comparison of approximate analytical result (dashed line) with numerical result (solid line). Analytical curve is given by $\Sigma_{\theta 3} = R^{-1/2}$ for $R > 1.59$ and $\Sigma_{\theta 3} = 0.863\, R^{-1/5}$ for $R < 1.59$. Arrows indicate creep zone boundary: num = numerical result; an = approximate analytical result. Creep exponent $n=4$.

Figure 3. Time-dependence of the amplitude of the HRR-near tip stress field, $A(t)$. The short-time limit (small scale yielding) is described by eq. (31). After long times (extensive creep of the whole specimen) the value given in eq. (12) is approached. The characteristic time, t_1 , is defined by equating long- and short-time solutions. Creep exponent $n=4$.

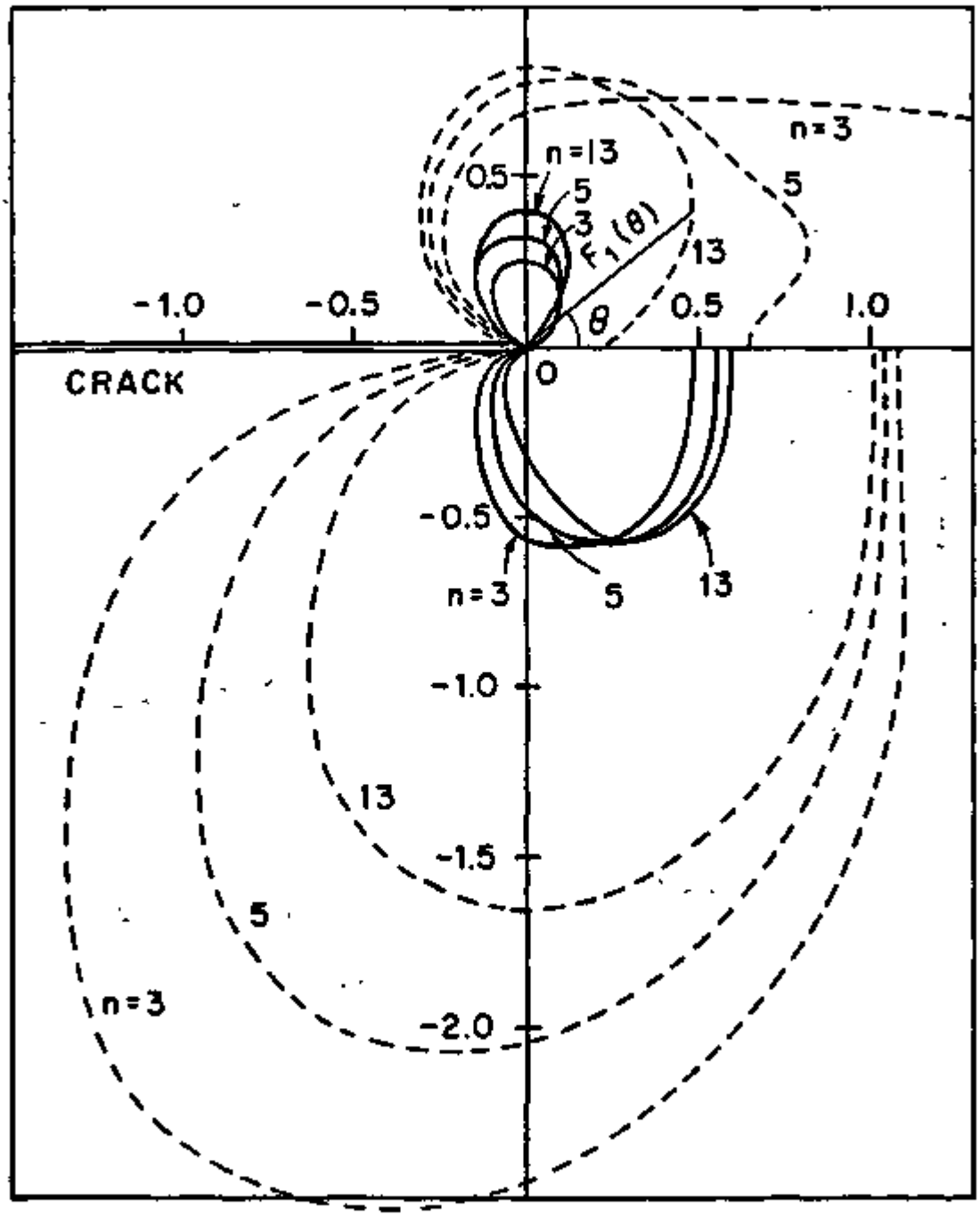
n=3
n=13
0.5
5
3
$f_1(\theta)$
13
5
-1.0
-0.5
θ
0.5
1.0
CRACK
0
-0.5
n=3
5
13
-1.0
13
-1.5
5
n=3
-2.0

Figure 1

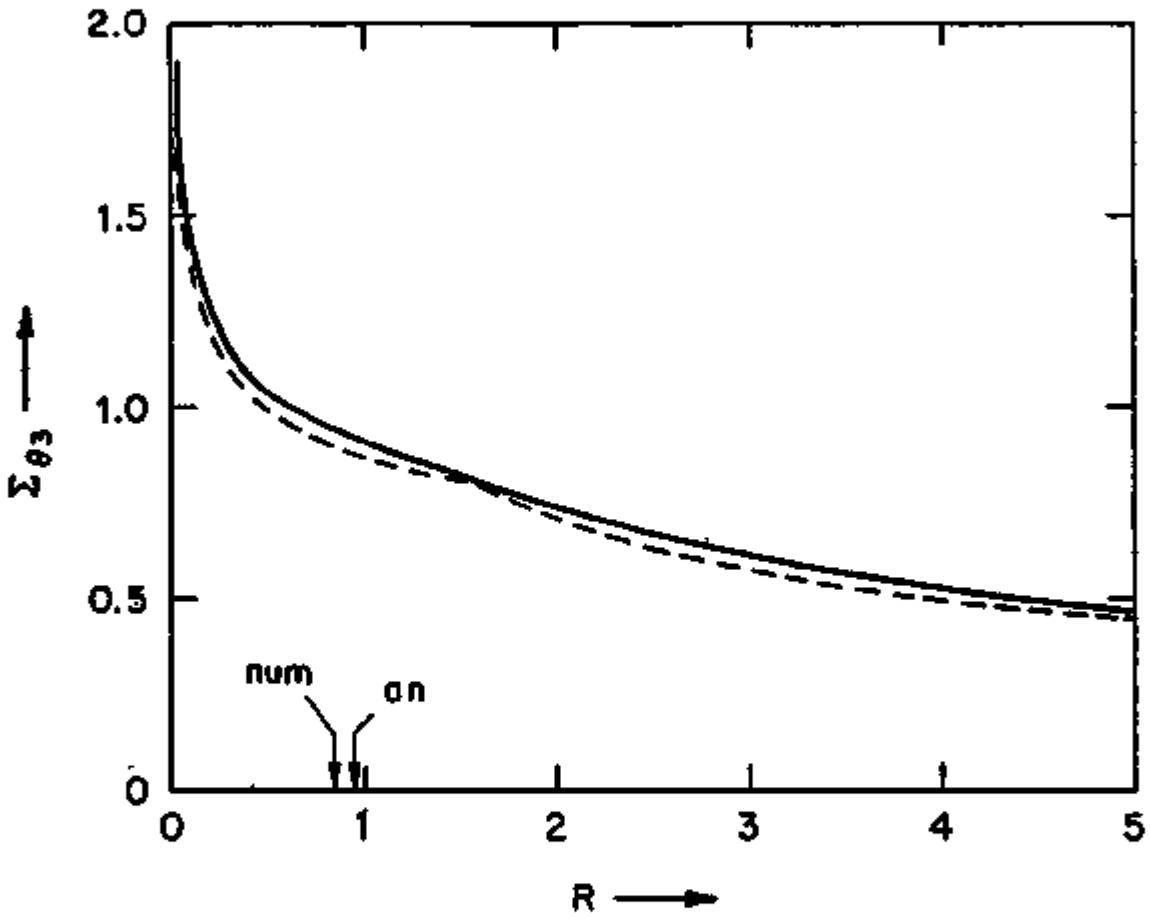

Figure 2

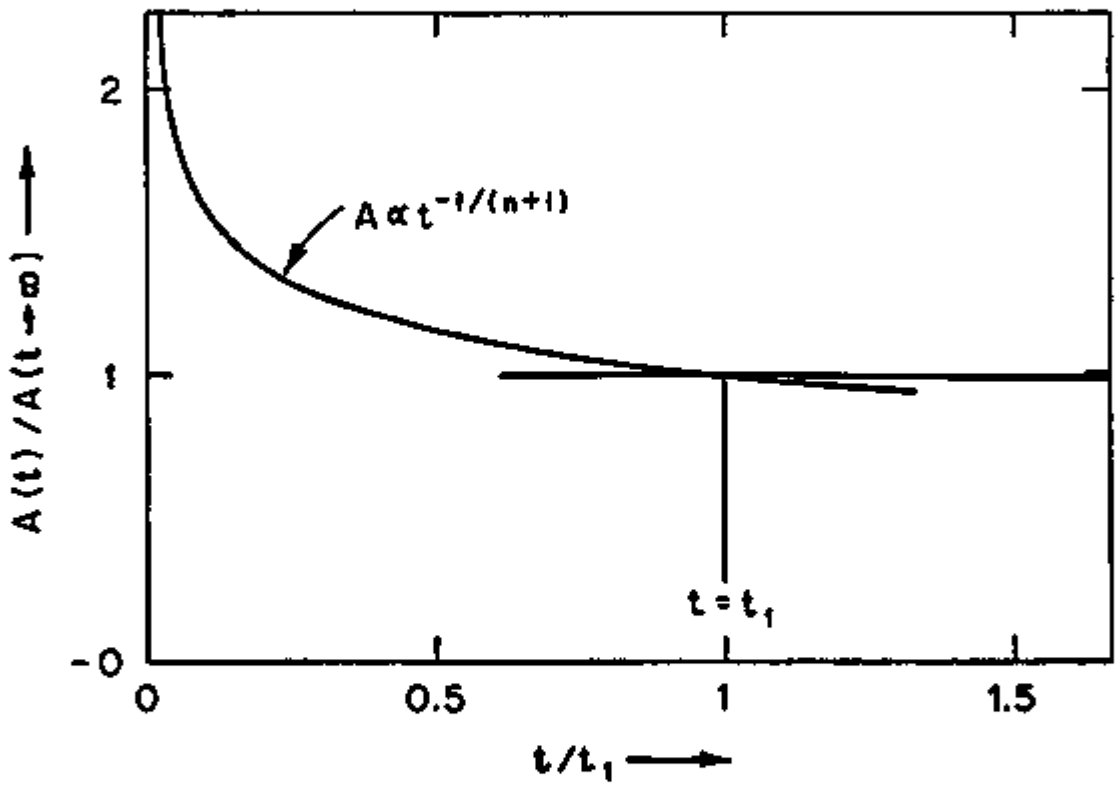

Figure 3